

Synthesis and Characterization of L-Threonine doped NiS Nanoparticle for Optoelectronic devices

Madhav N Rode, Vivek B.Kawade, Bhagwat R.Chavan

Abstract— L-Threonine doped NiS Metal Nanoparticle, a nonlinear optical materials has been synthesized by chemical route method. The synthesized materials were subjected to various characterization studies such as XRD, SEM, FTIR, and UV spectrum and powder nonlinear optical test. Optical behavior such as UV spectra and Second Harmonic Generation (SHG) was investigated to explore the NLO characteristics of the material. The NLO test was confirmed by Perry and Kurtz method. X-ray diffraction analysis revealed with that the morphology of the NiS: L-Threonine nanoparticles have Hexagonal structure. NiS: L-Threonine nanoparticles thus prepared 4nm to 2nm size. Morphology was determined by Scanning Electron Microscope (SEM), Fourier transform infrared spectroscopies has been performed which confirm the coordinates of compound.

Index Terms—Nanoparticle, XRD, UV spectra, NLO, L-Threonine

1 INTRODUCTION

NANOPARTICLES have attracted great interest in recent years because of their unique chemical, physical, optical, electrical and transport properties which are different from those of either the bulk materials or single atoms [1, 2]. Due to the vast surface area, all nanostructured materials possess a huge surface energy and thus are thermodynamically unstable or metastable. One of the great challenges in fabrication and processing of nanomaterials is to overcome the surface energy and to prevent the nanomaterials from growth in size driven by the reduction of overall surface energy. Due to high surface energy of the nanoparticles, they are extremely reactive and most systems without protection or passivation of their surfaces undergo aggregation [3]. This technology is sought to be the primary driver of the 21st century and the new economy [4, 5]. Knowledge in this new field of science is growing worldwide, leading to fundamental scientific advances. This will lead to dramatic changes in the ways that materials, devices, and systems are understood and created. Among the expected breakthroughs are an order of magnitude increase in computer efficiency, human organ restoration using engineered tissue, designer materials created from directed assembly of atoms and molecules and the emergence of entirely new phenomena in chemistry and physics [6]. Nanomaterials and most of the applications derived from them are still in an early stage of technical development. Much work still needs to be done in this newly born field of science. Nanoscience is the study of objects and systems in which at least one dimension is 1–100 nm. Nanosystems exhibit interesting and useful physical behaviours based on quantum phenomena. In recent

years, the preparations, characterizations, and applications of the nanosized materials have received great attention in various fields (Barnett and Landman 1997; Li et al. 1996; Han et al. 1997), e.g., chemistry, physics, material science, and biology. Since the nanoparticles usually have unusual electronic, optical, magnetic, and chemical properties significantly different from those of the bulk materials due to their extremely small sizes and large specific surface areas, they have various potential applications such as catalysis, electronic, optical and mechanical devices, magnetic recording media, superconductors, high-performance engineering materials, dyes, pigments, adhesives, photographic suspensions, drug delivery, and so on (Zhang and Mu 1994; Zhang and Cui 2000). Sulfide nanoparticles are a kind of inorganic nanoparticle which have been applied in many fields (Bianconi et al. 1991; Victor et al. 1997; Tsukasa 1999). Zhuang's group (2002) synthesized Ag₂S nanoparticles by homogeneous phase deposition and prepared silver ion-selective electrodes (ISEs). They also prepared CdS nanoparticles and cadmium ion-selective electrodes with the same method (Zhuang and Zhang 2004). [7]

Recently, it has been reported that nanostructure materials can be synthesized by mechanochemically induced solid-state displacement reactions [8-15]. The different phases of the NiS system have been the subject of many studies because of their applications like semiconductors and specially the metal-to semiconductor and paramagnetic antiferromagnetic first order transition at the same temperature of the h-NiS phase [16]. Between those applicabilities are rechargeable lithium batteries, solar cell storage, catalysis for hydrodesulphurization of petroleum products etc [17-18].

Sulfides of many transition metals show electronic and optical properties such as semiconductivity and photoconductivity [20, 21]. For example, nickel sulfide is a potential transformation toughening agent for semiconductor materials [22], while nickel disulfide adopts the pyrite structure and exhibits semiconducting properties [23]. Thus, the synthesis of the 3d transition metal sulfides has attracted great interests for sever-

- Madhav N Rode, M.Sc.Ph.D. Department of Physics, Vaidyanath College, Parli-Vajinath, Dist.Beed-431515, Maharashtra State, India, and Phone 02446 (222178). E-mail: madhav_rod@yahoo.co.in.
- Vivek B Kawade, M.Sc.Ph.D, Department of Physics, L.L.D Ladies College, Parli-Vajinath, Dist.Beed-431515 (M.S.) India.
- Bhagwat R. Chavn, M.Sc., Department of Physics, Swami Vivekanand College, Parli-Vajinath, Dist.Beed-431515, (e-mail: chavanbr@yahoo.co.in).

al decades. Normally, these sulfides are prepared through stoichiometric amount of the metal and sulfur heated in evacuated. However, the low melting point and volatilization of sulfur in some cases may make the control of composition difficult, and then several low temperature routes to group VIII transition-metal disulfides were recently reported [24-26]. For the preparation of sulfides of nickel, several techniques, such as solid-state reaction [27], chemical vapor transport [22, 28, 29], and liquid phase technique [22, 31], have been developed. It is reported that well-crystallized nickel sulfides could be obtained through the solvothermal technique, but the Na⁺ was easily adsorbed on the nanocrystallite to contaminate the product. Traditionally, NiS was prepared by solid-state reactions at high temperature and vapour phase reactions [32, 33]. Recently, many mild methods have been developed to prepare NiS. Henshaw et al. [34] and Dusastre et al. [35] reported room-temperature liquid ammonia route and room-temperature amine-assisted route to metal chalcogenides through elemental reactions, but the obtained nickel sulfide were amorphous. To obtain crystalline material, the heat treatment at 250–300 C is needed. The g-irradiation method was also used to prepare amorphous NiS, while a-NiS was obtained after claiming at 500 C [36]. Molecular precursor methods, including the thermal decomposition of compounds containing an M-S bond, have been thoroughly investigated and used to synthesize NiS usually at 300 C [37–39]. α-NiS and β-NiS were synthesized separately above 300 C by homogenous sulfide precipitation followed by a sulfurizing procedure through changing preparation conditions. In addition, Grau and Akinc [41, 42] reported precipitation of a-NiS from acidic solutions of thioacetamide in the temperature range of 70–90 C. But carbon contamination could not be avoided. NiS nanocrystals were prepared via a solvothermal reducing process with Zn as the reductant at 80–120 C in our lab [43]. In Present Paper we have synthesis NiS: L-Threonine material for Optoelectronic application. In the present paper we report the result of our synthesis nanostructure analysis of hexagonal NiS:L-Threonine and of investigation of its spectroscopic and nonlinear properties, XRD, UV spectra, SEM for optoelectronic applications.

2 EXPERIMENTAL SECTION

2.1 Synthesis

Nickel acetate (17.878 gm) was dissolved in 250ml of water with constant stirring Thiourea (7.612gm) was dissolved in 50ml sodium hydroxide (5 wt %) was dissolved in 10ml of deionized water. First Ni (ac)₂ solution and thiourea solutions were mixed together slowly with constant stirring. Faint green colour of Nickel acetate solution turned deep green by the addition of thiourea solution. Then NaOH solution was added to the original solution. The colour of the solution turned golden brown as the first drop of NaOH solution was added and the colour deepened with more of addition the colour turned to dark green. The solution was stirred for four Hours at 80°C. The solution of Na₂S was then added by drop with vigorous stirring to get NiS nanoparticles doped with molar% of

2%,4%,6% L-Threonine amino acid was added to the respective beakers of NiS:L-Threonine solution. (i.e. NiS: L-Threonine (1:0.02) NTh1, NiS: L-Threonine (1:0.04) NTh2, NiS: Threonine(1:0.06) NTh3).

2.2 CHARACTERIZATION

The Synthesis samples were subjected to powder X-ray diffraction analysis, NLO test, FTIR, TGA UV- spectra, SEM Characterization.

3 RESULT AND DISCUSSION

3.1 NLO TEST

The Second harmonic generation behavior was tested by Kurtz powder technique using Nd: YAG laser as a source. The sample was prepared by sandwiching the graded crystalline powder between two glass slides. The powder sample of NiS: L-Threonine was illuminated by the laser source (Wavelength= 1064nm) having pulse energy 2.35mJ, pulse duration 8 ns and repetition rate 10Hz has been used. The output has been measured at 532nm wavelength. The Second harmonic signal generated in the sample was collected by the lens and detected by the monochromator, which is coupled with the photomultiplier tube. The bright green emission was observed from the output of the powder form of the NiS: L-Threonine. KDP sample was used for the reference material and output power intensity of NiS: L-Threonine was comparable with the output power of KDP and it agrees well with the reported [44, 45]. The grown crystals have been subjected to the nonlinear optical study to measure the SHG efficiency with respect to the Pure KDP. To characterize the crystals, Kurtz and Perry method has been employed [46]. In this experiment Q-switched, mode locked Nd: YAG laser of wavelength 1064nm having pulse energy 3mJ/Pulse, pulse

Table 1:- Comparison of NLO property of various materials.

NLO Sample	Input	SHG output Signal in mV	SHG efficiency
KDPM1	2.50mJ/pulse	78mV	1.41
KDPM2	2.50mJ/pulse	85mV	1.54
KPN1	2.50mJ/pulse	102mV	1.85
KPN2	2.50mJ/pulse	95mV	1.72
KDP	2.50mJ/pulse/ 3 mJ/pulse	55mV / 65 mV	1
L-Alanine acetate [47]	2 mJ/pulse	16.5 mV	0.30
Ammonium borodilactate [48]	2 mJ/pulse	30.36 mV	0.552
L-Histidine bromide [49]	2 mJ/pulse	66 mV	1.20
L-Arginine diphosphate [50]	2 mJ/pulse	53.9 mV	0.98
Lithium para-nitrophenolate trihydrate [51]	2 mJ/pulse	93.5 mV	1.70
NiS:Th1	3 mJ/pulse	68.5 mV	1.053
NiS:Th2	3 mJ/pulse	70 mV	1.076
NiS:Th3	3 mJ/pulse	72.2 mV	1.110

duration 10ns and repetition rate 15Hz has been used. The output has been measured at 532nm wavelength. The increase in the SHG efficiencies are due to the weakening of the bond

between O-H and C=O due to hydrogen bonding [52, 53, 54].

3.2 X-RAY DIFFRACTION

As demonstrated in this document, the numbering for sections upper case Arabic numerals, then upper case. The grown crystals have been characterized by X-ray powder technique using Rich-Seifert X-ray powder diffractometer with Cu K α radiations of Wavelength (1.5406Å). The 2 θ range analyzed was from 10 °C to 70 °C employing reflection mode for scanning. The detector used was a scintillation counter in fig. represents the X-ray powder pattern for the synthesis NiS: L-Threonine (1:0.02) NTh1, NiS: L-Threonine (1:0.04) NTh2, NiS:L-Threonine(1:0.06) NTh3 metal nanoparticle. The X-ray diffractogram is shown in figure 1 to . The lattice parameters were calculated by using values of the high intensity peaks corresponding to the d-spacing and (hkl) Phases by computer programme POWD (Integrative powder diffraction and indexing programme). The XRD patterns are well matched to Hexagonal structure of NiS (JCPDS No-75-0613). Some differences such as the broadening of the diffraction peaks increasing or decreasing of some peaks intensity as well as the shift of the peaks position to slightly lower angles can be observed in spectra. In fact the intensities of the peaks in the host guest (Capped doped) Composite materials are increased with respect to those of Pure NiS . This increase of the peaks intensities can be related to the presence or incorporation of semiconductor inside the matrix structure. The X-ray diffraction patterns of NiS:L-Th1 (1:0.02) , NiS: L-Th2 (1:0.04), NiS:L-Th3 (1:0.06) nanoparticles are presented in Figure 1 to 3. The XRD data was analyzed by using PowderX software. The particle size of the synthesized nanoparticles was determined by using Debye-Scherer’s equation: $D = k \lambda / \beta \cos\theta$ Where, λ is the X-ray wavelength(1.54Å), k , the shape factor (0.94) , D , the average diameter of the crystals in Angstrom, θ , the Bragg angle in degree, and β is the line broadening measured by half-height in radians. The diffraction peaks for NiS at $2\theta = 22.313, 32.433, 38.64, 51.414, 58.55$ degrees, for NiS:Th1 at $2\theta = 32.105, 45.616, 52.57, 74.97$, for NiS:Th2 at $2\theta = 35.808, 45.625, 52.520, 70.689$ NiS:Th3 at $2\theta = 29.008, 36.683, 54.605, 64.622$ were chosen to calculate the size of the nanoparticles.

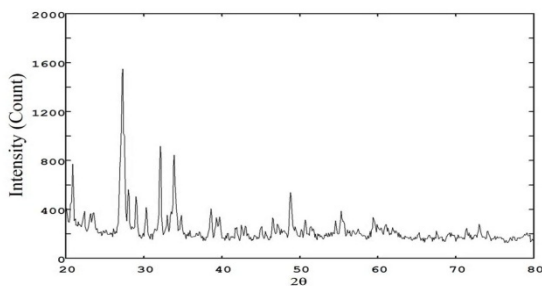


Figure 1: - XRD Spectrum of NiS: L-Th1

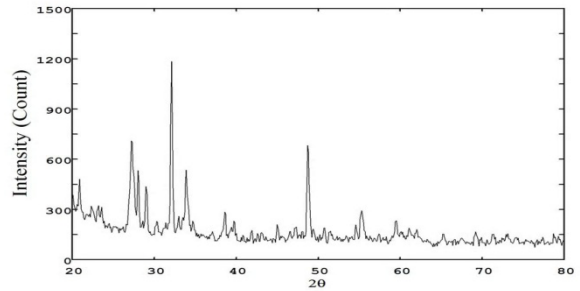


Figure 2: - XRD spectrum of NiS: L-Th2

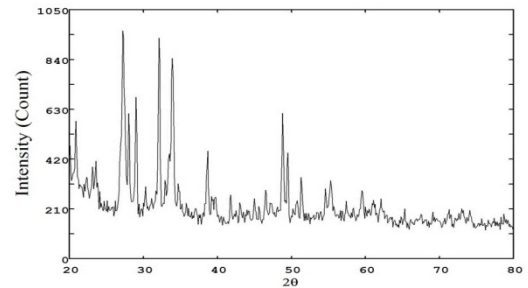


Figure 3: - XRD spectrum of NiS:L-Th 3

Tables 2:- XRD data ofr Pure and doped NiS

Samples	a	b	c
NiS	3.41705nm	3.41705nm	5.2891nm
NiS :Zn-Gly -2	3.41840nm	3.41840nm	5.2781nm
NiS :Zn-Gly -3	3.35473nm	3.35473nm	5.0334nm
NiS :Zn-Gly -4	3.31450nm	3.31450nm	5.1204nm
NiS:Th1	3.48501nm	3.48501nm	5.3775nm
NiS:Th2	3.41705nm	3.41705nm	5.28918nm
NiS:Th3	3.43216nm	3.43216nm	5.24910nm

Table 3:- Particle size of NiS doped L-Threonine

Sample	Particle size (nm)
NiS	4.05nm
NiS:Zn-Gly2	3.65nm
NiS:Zn-Gly3	2.85nm
NiS:Zn-Gly4	2.45nm
NiS:Th1	3.99nm
NiS:Th2	2.81nm
NiS:Th3	2.61nm

3.3 FTIR SPECTRA

The FT-IR spectrum of pure NiS and NiS: Th1, NiS: Th2, NiS: Th3 have been recorded on Perkin Elmer FT-IR spectrophotometer within the wave number range 600cm⁻¹ to 4000 cm⁻¹ Pellets of the mixture of each sample with KBr have been prepared and used in the experiment Figure 4. According to Nakamoto and Ferraro vOH in free water molecules appears

around 3600 to 3500 cm^{-1} , but in the present case the broad and strong band appeared at 2923 cm^{-1} , which is slightly lower than the expected. This may be possibly due to strong interaction between free water molecules. Another band, appearing at 1456 cm^{-1} may be assigned to δOH and also supports presence of free water molecules in crystal lattice as suggested [55]. IR also shows a strong band at 1152 cm^{-1} indicating the presence of SO_4^{2-} ion in the crystal structure as predicted [56].

uniform in size. The particle morphology observed was either hexagonal or cubic like shape.

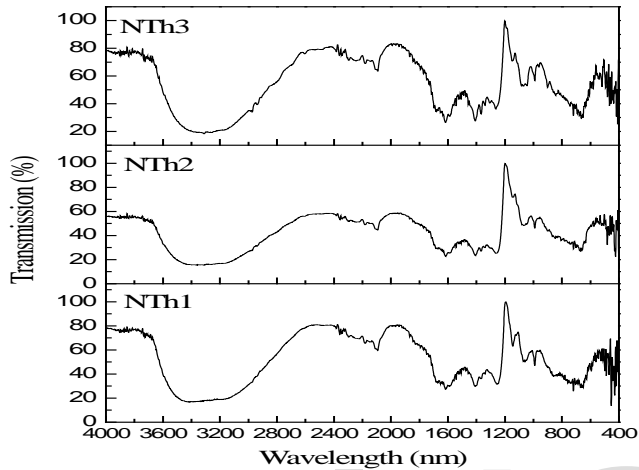


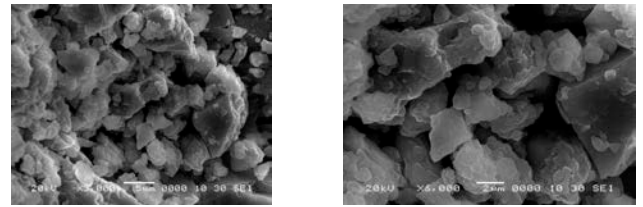
Figure 4: - FTIR Spectra of NiS:L-Th1,2,3.

3.4 SEM ANALYSIS

The particle size was confirmed by SEM image of the particles, which was recorded on the instrument JEOL-JSM-6380 Scanning Electron Microscope (Japan). The surface morphological features of synthesized nanoparticles were studied by SEM. Figure 6 to 7 shows the SEM image of synthesis samples with magnification of 3000 and 6000. The instrument parameters, accelerating voltage, spot size and magnification and working distances are indicated on SEM image. The results indicate that mono-dispersive and highly crystalline NiS, NTh1, NTh2, NTh3 nanoparticles are obtained.

The appearance of samples NiS, NTh1, NTh2, NTh3 particles is aggregated with bad size dispersion. We can observe that the particles are highly agglomerated and they are essentially cluster of nanoparticles. The Sample NTh 1, 2, 3 particles shows in the resulted in much aggregated particles despite the small crystallite size. We can observe that the use of sample NiS resulted in less aggregated and much better dispersed particles. The SEM picture indicates the size of polycrystalline particles. The observation of some larger nanoparticles may be attributed to the fact that NiS and other sample NZG nanoparticles have the tendency to agglomerate due to their high surface energy and high surface tension of the ultrafine nanoparticles. The fine particle size results in a large surface area that in turn, enhances the nanoparticles catalytic activity. So we can conclude that the prepared NiS and NZG particles are in nanometer range. The average diameter of the particle observed from SEM analysis is 40nm to 25nm, which is larger than the diameter predicted from X-Ray broadening. From the micrograph, it was observed that the nanoparticles are almost

Figure 5:



SEM of NiS: L-Th1

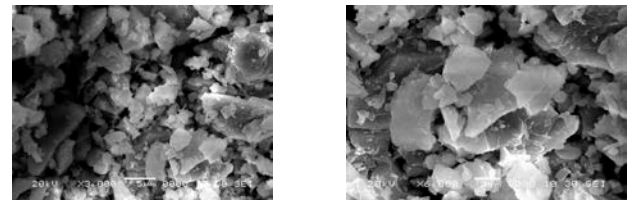


Figure 6: SEM of NiS: L-Th2

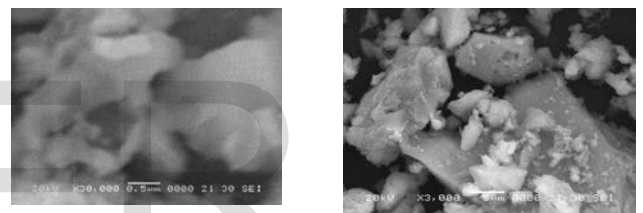


Figure 7: SEM of NiS: L-Th3

3.4 UV SPECTRA

The UV-Vis Spectral studies were carried out by using JASCO UV-Vis-NIR spectrometer, model name V-670 in the range 200nm - 800nm and Band width (UV/Vis) 200nm and Band-width (NIR) 20nm and it shown in fig 8. The NZG has a good transmittance and the lower cut off wavelength is 200nm. The reflectance % show that the decay trends 250nm to 800nm range good visible region. The large transmission in the entire region enables it to be a good candidate for optoelectronic application. Reflectance peak corresponding to the fundamental reflection appears at 232nm for pure NiS, 219.5 for NiS: L-Th1, 213.5 for NiS:Th2, 218.5nm for NiS:Th3. The shifting of peaks shows the good transparency. After that between the range of 438nm to 800nm (NiS); 305 to 800nm (NTh1); 312 to 800nm (NTh2); 312nm to 800nm (NTh3) the material is observed to be transparent and the reflectance is less and insignificant. The less reflectance in these regions is important for the material possessing NLO properties. The steep increase in reflectance below 219 nm is due to the colour of the synthesis materials in and beyond the visible region. From the spectra with the increase in the dopant concentration there is decrease in the reflectance, this might be due to the absorption energy level introduced by dopant. NiS is known as photoluminescence quencher hence there is increase in the reflectance. With further increase in the doping concentration but NiS:L- Th3 there

is decrease in the reflectance because NiS introduces new energy level in the band structure. It acts as electron trapping center which results into nonradiative recombination. Therefore, reflectance decrease as the molar concentration of dopant increases.

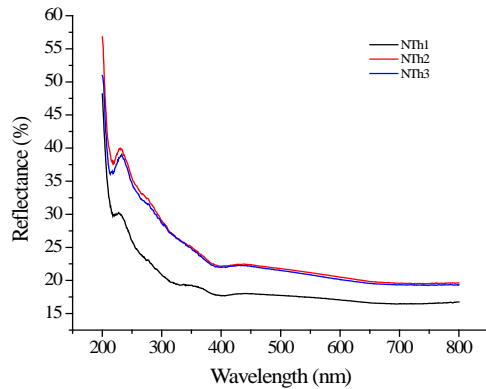


Figure 8: UV Spectra of NiS: L-Th1, NiS: L-Th2, NiS: L-Th 3

4 CONCLUSION

NiS doped L-Threonine doped have been successfully prepared by chemical route method. The method of preparation is inexpensive easy and environmental friendly. The NLO test confirms the naocrystal may be used for optoelectronics. X-ray diffraction analysis revealed that the morphology of the NiS:L-Threonine nanopartilces has hexagonal structure with an average particle size 2.5 nm. FT-IR spectroscop confirms the formation of the expected compound. UV- Visible spectroscopic study confirms the increase in band gap.

REFERENCES

[1] W. Dong, C. Zhu, *Opt. Mater.* **22**, 227 (2003).
 [2] A.D. Yoffe, *Adv. Phys.* **42**, 173 (1993).
 [3] A. Vllman, *Chem. Rev.* **96**, 1533 (1996).
 [4] K.P. Chong, *J. Physics and Chemistry of Solids*, **65** (2004) 2.
 [5] A.L. Rogach, A. Eychmuller, S.G. Hickey and S.V. Kershaw, *Reviews; Infrared emission*, www.small-journal.com, small 2007, 3 (4) 536.
 [6] M.C. Roco and W.S. Bainbridge, *Societal Implications of Nanosciences and Nanotechnology*, (Springer, Boston) 2001
 [7] Li.Liu and Lei Wang, *Analytical Letter*,**39**:879-890,2006.
 [8] A.Dodd and P.G.Mc Cormick,*Scripta Mater.***44**(2001)1725.
 [9] P.Balaz, E.Boldizarova, E.Godocikova and J.Briancin; *Mater.Lett.***57** (2003) 1585.
 [10] M.Achimovicova, E.Godocikova, P.Balaz, J.Kovac, A, Saka and P.Billik, *Acta.Metall.Slovaca*, **11**(2005)145.
 [11] T.Tsuzuki and P.G.Mc Cormick, *Appl.Phys.A***65** (1997)607.
 [12] T.Tsuzuki and P.G.McCormick, *J.Mater.Sci.*(**39**) (2004),5143.
 [13] F.Sato, Q.Zhang and J.Kano, *J.Mater.Sci.* (**39**)2004)5051
 [14] P.G.McCormick, T.Tsuzuki, J.S.Robinson and J.Ding, *Adv.Mater.***613** (2001) 1008.
 [15] J. T. Sparks, T. Komoto, *Rev. Mod. Phys.* **40**, 752 (1968).
 [16] J. Wang, S. Y. Chew, D. Wexler, G. X. Wang, S. H. Ng, S. Zhong, H. K. Liu, *Electrochem. Commun.* **9**, 1877 (2007).

[17] J. T. Kloprogge, W. J. J. Welters, E. Booy, V. H. J. de Beer, R. A. van Santen, J. W. Geus,
 [18] J. B. H. Jansen, *Appl. Catal. A: Gen.* **97**, 77 (1993).
 [19] A. M. Fernandez, M. T. S. Nair, P. K. Nair, *Mater. Manuf. Processes* **8**, 535(1993)
 [20] Q.Y. Lu, J.Q. Hu, K.B. Tang, et al., *J. Solid State Chem.*, **1999**, **146**, 484.
 [21] Y.U. Jeong, A. Manthiram, *Inorg. Chem.*, **2001**, **40**, 73.
 [22] J. Grau, M. Akinc, *J. Am. Ceram. Soc.*, **1997**, **80**, 941.
 [23] A. Manthiram, Y. U. Jeong, *J. Solid State Chem.*, **1999**, **147**, 679.
 [24] X. M. Zhang, X. F. Qian, C. Wang, et al., *Mater. Sci. Eng.*, **1999**, **B57**, 170.
 [25] J. D. Passaretti, R. B. Kaner, R. Kershaw, et al., *Inorg. Chem.*, **1981**, **20**, 501.
 [26] J. D. Passaretti, R. C. Collins, A. Wold, *Mater. Res. Bull.*, **1979**, **14**, 1167.
 [27] P. R. Bonneau, R. K. Shiao, R. B. Kaner, *Inorg. Chem.*, **1990**, **29**, 2511.
 [28] A. Olivas, J. Cruz-Reyes, M. Avalos, et al., *Mater. Lett.* **1999**, **38**, 141.
 [29] J. Grau, M. Akinc, *J. Am. Ceram. Soc.*, **1996**, **79**, 1073.
 [30] R. J. Bouchard, *Mater. Res. Bull.*, **1968**, **3**, 563.
 [31] X. F. Qian, Y. D. Li, Y. Xie, et al., *Mater. Chem. Phys.*, **2000**, **66**, 97.
 [32] R. Coustal, *J. Chem. Phys.* **38**,1958. 277.
 [33] D. Delafosse, P. Barret, *C. R. Acad. Sci.* **252**,1961. 888.
 [34] G. Henshaw, I.P. Parkin, G.A. Shaw, *J. Chem. Soc., Dalton Trans.*,**1997**. 231.
 [35] B.O. Dusastre, I.P. Parkin, G.A. Shaw, *J. Chem. Soc., DaltonTrans.* **3505**,1997..
 [36] G.Z. Bian, Y.D. Yin, Y.L. Fu, Z.H. Wu, T.D. Hu, T. Liu, *Acta. Phys.-Chim. Sin.* **16**, 2000. 55.
 [37] D.M. Wilhelmy, E. Matijevic, *J. Chem. Soc., Faraday Trans.***563**,1984..
 [38] P. Roman, J.I. Beitia, A. Lague, *Polyhedron* **14**, 1995. 2925.
 [39] H. Tomesz, J.K. Jan, C. Ewe, K. Tadeusz, *J. Electroanal. Chem.* **367**, 1994. 212.
 [40] A. Olivas, J. Cruz-Reyes, M. Avalos, V. Petranovskii, S.Fuentes, *Mater. Lett.* **38**, 1999. 141.
 [41] J. Grau, M. Akinc, *J. Am. Ceram. Soc.* **79**, 1996. 1073.
 [42] J. Grau, M. Akinc, *J. Am. Ceram. Soc.* **80**, 1997. 941.
 [43] X.M. Zhang, C. Wang, Y. Xie, Y.T. Qian, *Mater. Res. Bull.* **34**, 1999. 1967.
 [44] Misoguti, L ; Varela,A ; Nunes,F.D.;Bagnato,V.S.;;Melo.F.E.A.;Mendes Filho,J;;Zilio,S.C. *opt.Mater.***1996**,**6**,147-152.
 [45] Raxxeti,C;;Ardoino,M.Zanotti,L;Zha,M;; Paorici,C.*Cryst.Res.Technol* **2002**,**37**,456-465.
 [46] S.K.Kurtz, T.T.Perry, Jr.*Appl. Physics* **39** (1968) 3798.
 [47] G.Ramesh Kumar, S.Gokul Raj, R.Mohan, R.Jayavel, Jr.*crystal growth* **283** (2005) 193.
 [48] S.Dhanskadi, P.A.Angeli Mary, Jr.*crystl. Growth* **253** (2003) 424 - 428.
 [49] B.Milton Boaz, S.Jeome Das, Jr.*crystl. Growth* (279) (2005) 383 - 389.
 [50] Ra.Shanmugavadivu, Gravel, A.Nixon Azariah, *Journal of physics and chemistry of solids* **67** (2006)1861.
 [51] D.Prem, Anand, M.Gulam Mohamed, S.A.Rajasekar, Seselwa kumar, A. Joseph, Arul Aragasam, P.Sagayaraj. *Material Chem. & Physics* **97** (2006) (510 - 505).
 [52] A. Olivas, J. Cruz-Reyes, M. Avalos, et al., *Mater. Lett.*, **1999**, **38**, 141.
 [53] J. Grau, M. Akinc, *J. Am. Ceram. Soc.*, **1996**, **79**, 1073.
 [54] R. J. Bouchard, *Mater. Res. Bull.*, **1968**, **3**, 563.
 [55] X. F. Qian, Y. D. Li, Y. Xie, et al., *Mater. Chem. Phys.*, **2000**, **66**, 97.
 [56] R. Coustal, *J. Chem. Phys.* **38**,1958. 277.

IJSER